Journal of Inflammation Research

Dovepress
open access to scientific and medical research

Open Access Full Text Article

ORIGINAL RESEARCH

Significance of Immunogenic Cell Death-Related Prognostic Gene Signature in Cervical Cancer Prognosis and Anti-Tumor Immunity

Shan Jiang[1,2], Zhaolei Cui[3], Jianfeng Zheng[1], Qiaoling Wu[1], Haijuan Yu[1], Yiqing You[3], Chaoqiang Zheng[3], Yang Sun[1]

[1]Department of Gynecology, Clinical Oncology School of Fujian Medical University, Fujian Cancer Hospital, Fuzhou, 350014, People's Republic of China; [2]College of Integrative Medicine, Fujian University of Traditional Chinese Medicine, Fuzhou, 350122, People's Republic of China; [3]Laboratory of Biochemistry and Molecular Biology Research, Department of Clinical Laboratory, Clinical Oncology School of Fujian Medical University, Fujian Cancer Hospital, Fuzhou, 350014, People's Republic of China

Correspondence: Yang Sun, Department of Gynecology, Clinical Oncology School of Fujian Medical University, Fujian Cancer Hospital, No. 420 Fuma Road, Fuzhou, Fujian, 350014, People's Republic of China, Email sunyang@fjzlhospital.com

Background: Immunogenic cell death (ICD) can reshape the immune microenvironment of tumors. Driven by stressful pressure, by directly destroying tumor cells and activating the body's adaptive immunity, ICD acts as a modulator of cell death, enabling the body to generate an anti-tumor immune response that produces a more effective therapeutic effect, while tumor cells are driven to kill. Hence, this research aimed to find and evaluate ICD-related genetic signatures as cervical cancer (CC) prognostic factors.

Methods: Data of CC patients from the Tumor Genome Atlas (TCGA) were used as the basis to obtain immunogenic cell-death-related prognostic genes (IPGs) in patients with CC, using the least absolute shrinkage and selection operator and Cox regression screening, and the IPGs scoring system was constructed to classify patients into high- and low-risk groups, with the Gene Expression Omnibus (GEO) dataset as the validation group. Finally, the difference analysis of single-sample gene set enrichment analysis, tumor microenvironment (TME), immune cells, tumor mutational burden, and chemotherapeutic drug sensitivity between the high-risk and low-risk groups was investigated.

Results: A prognostic model with four IPGs (PDIA3, CASP8, IL1, and LY96) was developed, and it was found that the group of CC patients with a higher risk score of IPGs expression had a lower survival rate. Single and multifactor Cox regression analysis also showed that this risk score was a reliable predictor of overall survival. In comparison to the low-risk group, the high-risk group had lower TME scores and immune cell infiltration, and gene set variation analysis showed that immune-related pathways were more enriched in the high-risk group.

Conclusion: A risk model constructed from four IPGs can independently predict the prognosis of CC patients and recommend more appropriate immunotherapy strategies for patients.

Keywords: ICD, cervical cancer, immunity, prognosis, immunotherapy response

Introduction

One of the top four causes of mortality for women globally and one of the four most prevalent malignancies in women is cervical cancer.[1] Surgery, radiation, and chemotherapy are the major treatments for advanced CC; however, owing to tumor recurrence and metastasis, the prognosis for these patients is very poor.[2] Therefore, it is critical to urgently search for changes in the factors associated with CC prognosis and the molecular mechanisms involved to provide effective treatment and improve patient prognosis.

Immunogenic cell death (ICD) is activated by stress-driven activation, such as chemotherapeutic agents or physiotherapy modalities, enhancing tumor immunogenicity, recruiting dendritic cells (DCs) to the tumor and driving their anti-tumor effects, and activating specific cytotoxic T lymphocyte (CTL) attack on the tumor.[3] ICD can be considered

Received: 6 March 2023
Accepted: 5 May 2023
Published: 22 May 2023

a new way to treat tumors: cancer cells killed by chemotherapy and radiotherapy can activate ICD, allowing the body's CTL to perform cancer cell clearance again; in addition, ICD can also reduce drug resistance produced by tumors and enhance CTL anti-tumor immunity via ICD-mediated immune response.[4] Moreover, there are ICD-based anti-cancer drugs, such as FDA-approved belantamab mafodotin, for treating patients with relapsed or refractory multiple myeloma and lurbinectedin for the treatment of metastatic small-cell lung cancer.[5,6] However, the immune microenvironment of ICD involved in CC remains unknown. Therefore, we examined ICD-related genes with significant prognostic value in this investigation. Prognostic features were developed based on four ICD-associated genes (PDIA3, CASP8, IL1B, and LY96), and patients were classified into high-risk and low-risk groups based on the features to explore differences in prognosis, enrichment pathways, immune microenvironment, immunotherapy, and drug sensitivity between high-risk and low-risk groups.

Materials and Methods

To make our entire study easier to understand, we made a flowchart as shown in Figure 1.

Dataset and Preprocessing

In this study, RNA sequencing data from 309 samples in the Cancer Genome Atlas (TCGA) database (https://tcga-data.nci.nih.gov/tcga/) and patient samples in the Gene Expression Omnibus (GEO: GSE44001, GSE168652, GSE6791) database (http://www.ncbi.nlm.nih.gov/geo/) and their patients with complete gene expression data and clinical prognosis information were removed to carry out following analysis. Fragments per kilobase of transcript per million fragments mapped values were converted to transcripts per million values for analysis to reduce cross-sample inaccuracies in sample quantification.[7] From previous literature and studies, 49 genes associated with ICD were obtained.[8–12]

Gene Set Variation Analysis

The "RCircos" R package was used to analyze the frequency of copy number variant (CNV) gain or deletion in 49 related genes on 23 pairs of human chromosomes to analyze the mutations of ICD-related genes in CC.[13] The mutation frequency, mutation type, and base changes of ICD-related genes in the TCGA cohort were investigated using the "maftools" R package.[14]

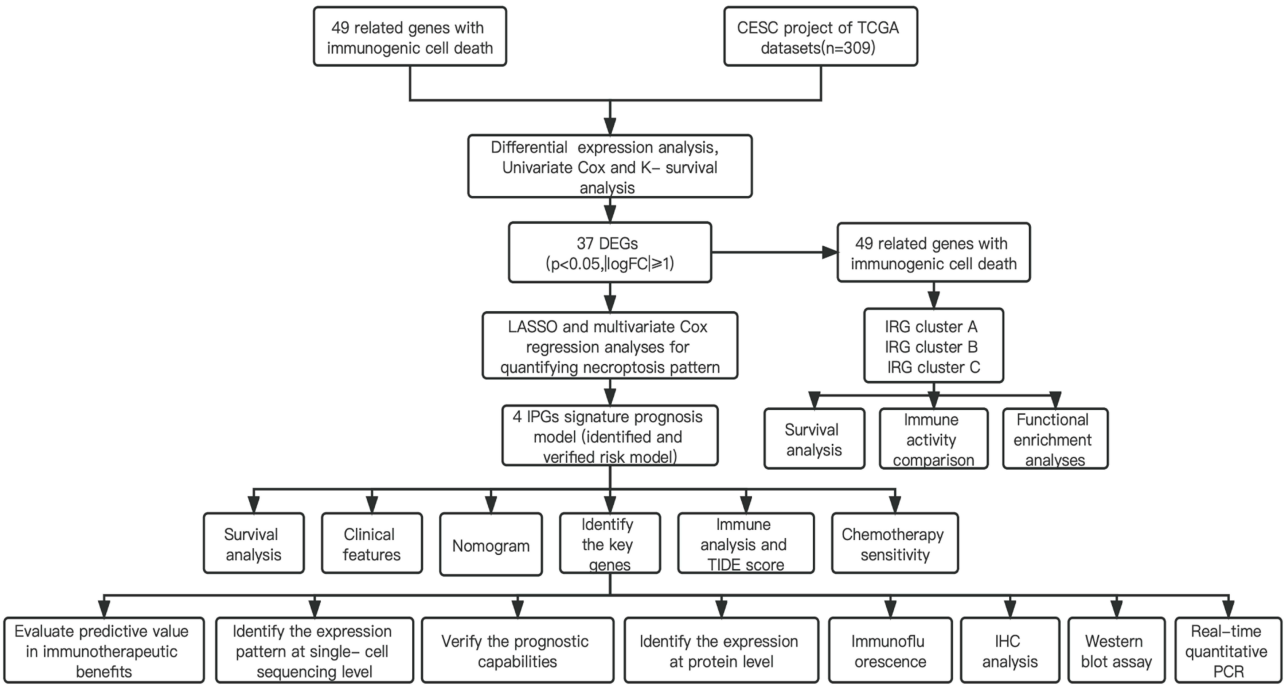

Figure 1 Flow chart of this study.

IRG Expression-Based Clustering Grouping

Using the R package "ConsencesclusterPlus",[15,16] tumor samples were stratified and clustered based on the expression of ICD-related genes in CC samples. Prognostic differences between groups were analyzed using Kaplan–Meier (K-M) curves, and principal component analysis was used to validate the reliability of the clustering analysis. Gene Ontology (GO) and Kyoto Encyclopedia of Genes and Genomes (KEGG) enrichment analyses were performed to investigate the biological differences between different groups, and differences in pathway enrichment were analyzed between groups. The r package "clusterProfiler" carried out an analysis of the functional annotations from the Gene Ontology (GO) and Kyoto Encyclopedia of Genes and Genomes (KEGG) databases.[17]

Construction of a Risk Score Model Related to ICD

The expression of ICD survival-related genes was determined using the "limma" R package.[18] The R package "glmnet" was used to narrow down the candidate genes using the least absolute shrinkage and selection operator (LASSO) and Cox regression.[19,20] The risk score of the IPGs model was calculated as follows: RiskScore = $\sum$(Expi $*$ Coefi), where Coefi represents the risk coefficient and Expi represents gene expression.[21] ROC curve and AUC evaluation with the "survivalROC" R program.[22] The receiver operator characteristics (ROC) curves were used to determine the risk model accuracy. Univariate and multivariate Cox regression analyses were conducted together with clinical data to ascertain if the risk score may be used as an independent predictive predictor of prognosis in patients with CC. Threshold values were established utilizing the "maxstat" R package to define prognostically meaningful high- and low-risk groups.[23]

The Correlation Analysis Between IRG and Immune Infiltrating Cells and Immunotherapy Prospects

This was achieved using the "ESTIMATE" R package.[24,25] The ImmuneScore, StromalScore, and ESTIMATEScore were calculated, representing the immune infiltration score, stromal cell infiltration score, and the estimated score, which is a combination of the stromal cell and immune cell scores. The degree of immune cell infiltration in different groups was assessed using a single-sample gene set enrichment analysis (ssGSEA).[26] The "pRRophetic" package was used to calculate drug sensitivity differences between risk groups.[27] We also used the Tumor Immune Dysfunction and Exclusion (TIDE) (http://tide.dfci.harvard.edu/) algorithm to predict the effects of immunotherapy in different risk groups of patients.

Experimental Materials

The human CC-related cell lines HeLa and C33a were purchased from Meisen (Zhejiang, China), and SiHa and ME180 were purchased from Pricella (Wuhan, China). All cultures were supplemented with RPMI 1640 medium, 0.25% trypsin ethylenediamine tetraacetic acid, and fetal bovine serum (Gibco, NY, USA) and maintained below 5% CO_2 at 37 °C. PDIA3 antibody (Proteintech, Wuhan, China), GAPDH antibody (CST, Shanghai, China), goat anti-rabbit IgG antibody secondary antibody (Zsbio, Beijing, China), and goat anti-mouse IgG H&L/Cy3 (Beyotime, Shanghai, China).

Immunofluorescence

For PDIA3 co-localization analysis, the CC cells were treated with a PDIA3 antibody (1:2000 dilution) overnight at 4 °C. The cells were then restained with goat anti-rabbit IgG H&L/FITC (1:2000 dilution).

Western Blot

The total protein concentration of CC cells was determined using the BCA protein concentration assay kit. A total of 20 μg protein loading volume was separated by 10% SDS polyacrylamide gel electrophoresis, transferred to polyvinylidene fluoride (PVDF) membrane, and closed with TBST solution containing 5% BSA at room temperature. After that, the membrane was incubated with diluted antibodies PDIA3 (1:2000) and GADPH (1:2000) at 4°C overnight, respectively. Finally, the samples were re-incubated with goat anti-rabbit IgG antibody secondary antibody (1:5000) at room temperature for 1 h, washed three times with TBST, and developed by enhanced chemiluminescence (ECL).

Immunohistochemistry

We collected 8 pairs of cervical cancer tissues matched with their adjacent normal tissue samples at Fujian Provincial Cancer Hospital. The use of cervical cancer specimens for this study was approved by the ethics committee of Fujian Cancer Hospital. Informed consent was signed after the patients were fully informed of the purpose of the study. The tissues were routinely dewaxed with water, washed with PBS, treated with methanol solution at room temperature for 10 min, washed again with PBS, and the citric acid antigen repair solution was boiled for 10 min, then moved to room temperature and cooled at rest. Blocking Buffer for 10 min. The diluted primary antibody was incubated at 4 °C overnight, and the diluted secondary antibody was incubated at room temperature for 1 h. Finally, the AEC chromogenic kit was used for 10 min, then the sections were rinsed with distilled water, counterstained with hematoxylin for 3 min, sealed with water-soluble tablets, and observed under the microscope after drying.

Real-Time Quantitative PCR

After receiving approval from the Fujian Cancer Hospital's Ethics Committee, we obtained 8 normal ovarian tissues and 24 samples of CESC tissue to perform quantitative real-time PCR (qPCR). Utilizing the Total RNA Extraction Kit from Promega, total RNA was extracted from the tissue samples (Shanghai, China). After RNA extraction, we produced cDNA by reverse transcribing whole RNA using the Transcriptor First Strand cDNA Synthesis Kit in Shanghai, China. We used SuperReal PreMix Plus from Tiangen Biotech to conduct qPCR to determine the expression level of IPGs in the signature (Beijing, China). The sequences of the IPGs primers that we bought from Sangon Biotech in Shanghai, China, are reported in Supplementary Table 1.

Statistical Analysis

R software (version 4.1.3) was used for statistical analysis. We compared overall survival between high-risk and low-risk groups using K-M analysis with the Log-rank test. The Mann–Whitney test was used to compare immune cell ssGSEA scores and immune-related pathways between groups. Two-tailed p-values < 0.05 were considered statistically significant.

Results

Inheritance and Mutation of IRG in CC Samples

Based on previous ICD literature reports, 49 IRG were included in this study. Presentation of the top 15 differentially expressed genes based on IRG mRNA expression levels in normal and cervical cancer tissues in the TCGA dataset, where genes with higher amplification frequencies of BAX, CASP8, and CALR were also significantly more expressed in cancerous tissues (Figure 2A).

The genes with a high copy number amplification frequency included PIK3CA, TNF, SLAMF7, and NLRP3, while those with a high copy number deletion frequency included HMGB1, CASP8, CASP1, and PDIA3 (Figures 2B and D). We found that 130 of 289 CC samples had mutations in IRG, with a mutation frequency of 44.98%. The PIK3CA gene had the highest mutation frequency, followed by CDK12, CASP8, and IFNGR1 genes (Figure 2C). Furthermore, we investigated the role of IRG in CC prognosis, and most of the associated genes had the same impact on CC prognosis. For example, the adverse factors PDIA3, ATG5, CD8B, and IL10 were positively associated (Figure 2E).

Analysis of Immune Cell Infiltration Characteristics of Different Groups Based on IRG Expression Clustering

We performed IRG expression-based clustering analysis of CC patients in the TCGA dataset using the R package "ConsenceclusterPlus" to further investigate IRG. When the CC samples were divided into groups A, B, and C, testing with k = 2–9 revealed that k = 3 had the best cluster stability. The best groupings had higher partial correlations within groups and lower correlations between groups (Figures 3A and Supplementary Figure 1).

Heat maps were then used to compare IRG expression levels across the three groups, and the results revealed that most IRG expressions were upregulated in clustered groups A and B. Both groups A and B had a worse prognosis than group C (Figures 3B and C). ssGSEA revealed significant differences in the content of 29 immune cells between the three

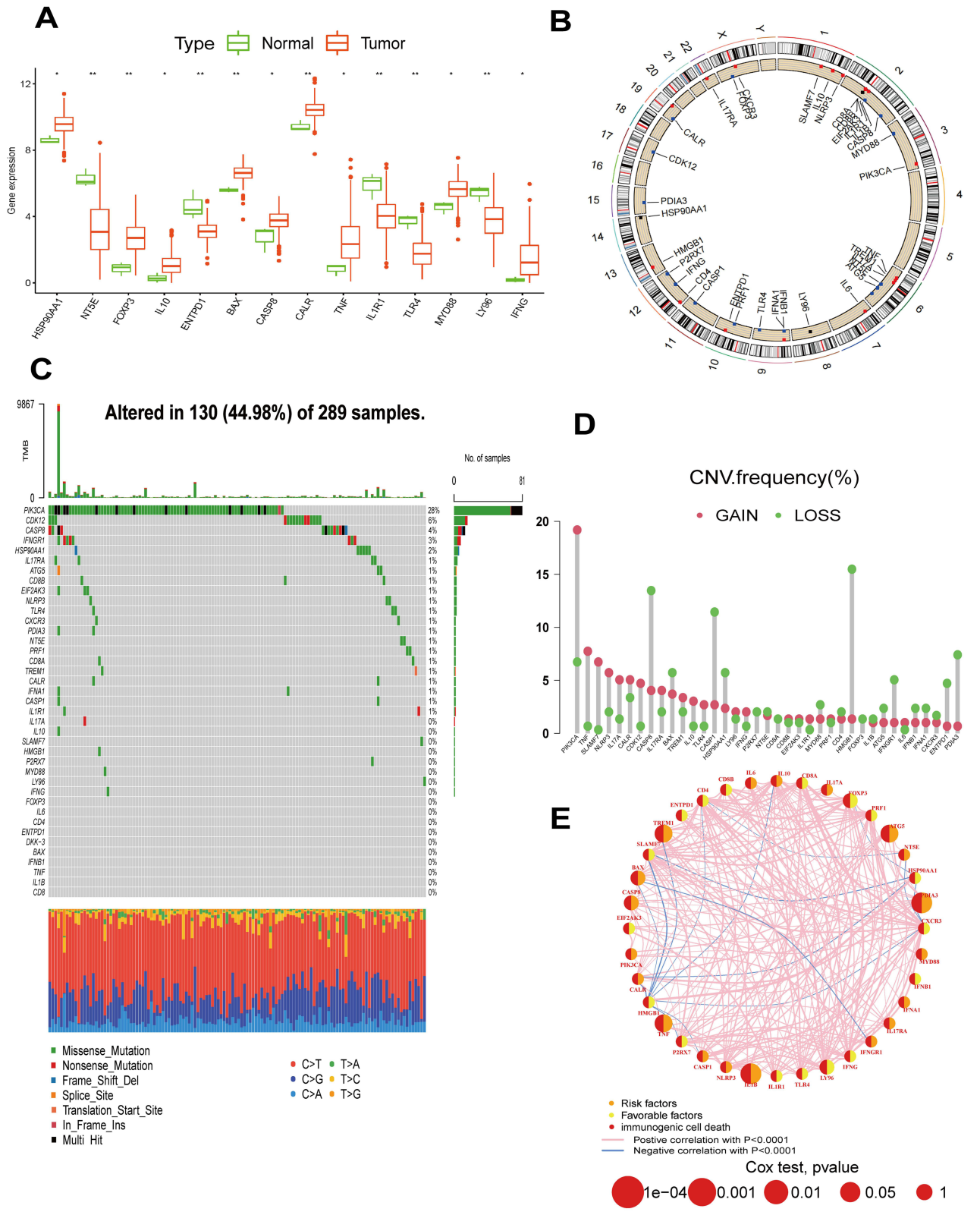

Figure 2 Genetic and variant expression of immunogenic death-related genes (IRG). (**A**) Differences in IRG expression in normal and cervical cancer (CC) tissue samples (*p < 0.05 and **p < 0.01). (**B**) IRG copy number variants (CNVs) localized on 23 chromosomes. (**C**) IRG mutation frequencies in 289 CC patients, with different colors corresponding to mutation types at the bottom of the graph. (**D**) IRG CNV frequencies in CC samples. (**E**) IRG interaction in CC samples.

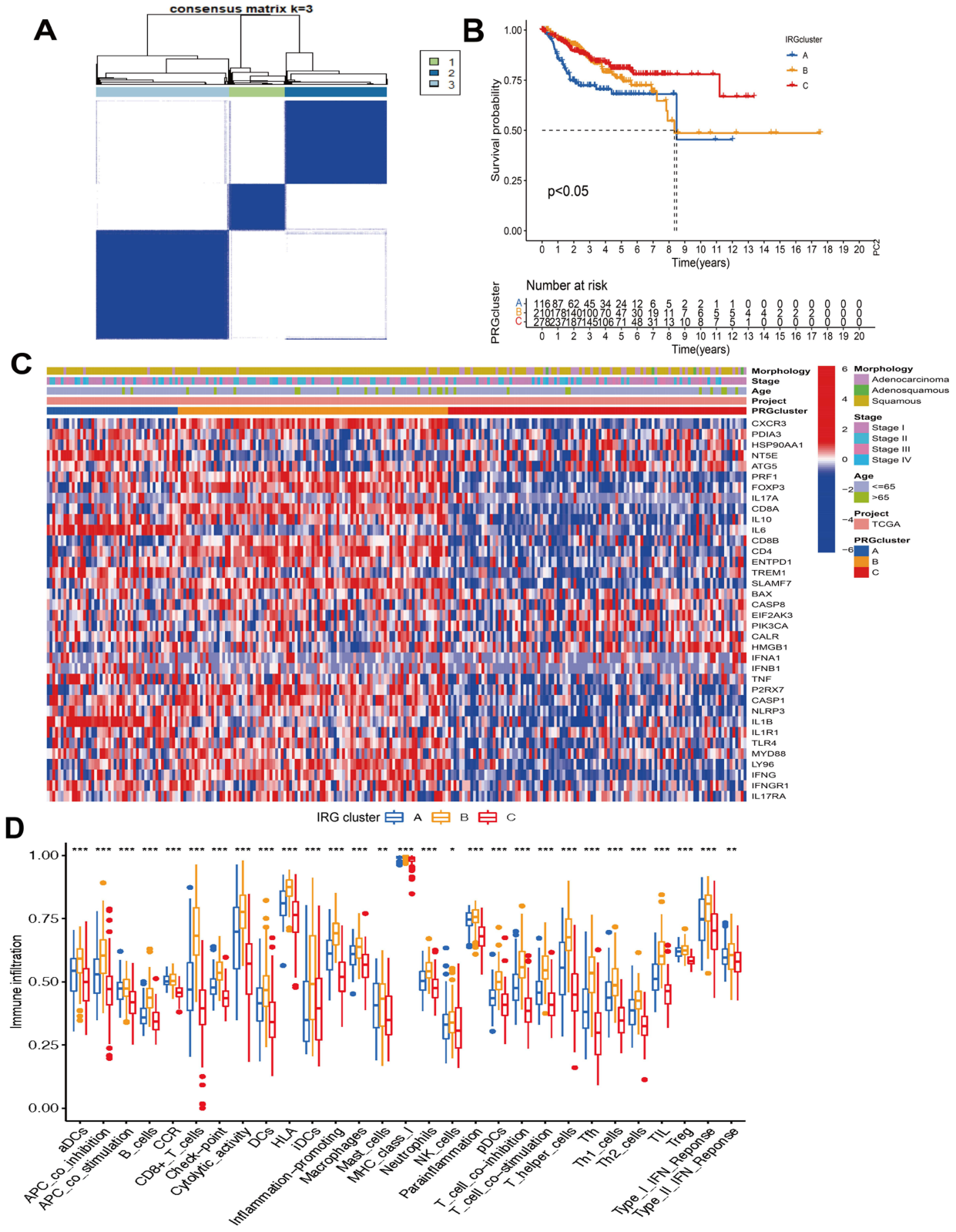

Figure 3 Consensus clustering analysis based on immunogenic death-related genes (IRG) expression. (**A**) IRG clustering grouping of all samples (k = 3). (**B**) Survival differences in IRG clustering groups. (**C**) Heat map of IRG expression in different clustering groups. (**D**) The abundance of each immune cell in IRG clustering groups (*p < 0.05, **p < 0.01, and ***p < 0.001).

groups, with both groups A and B showing a high infiltration of immune cells, primarily immunosuppressive cells such as macrophages, mast cells, and regulatory T cells (Figure 3D).

The Biological Behavior of DEGs in Different Clustering Groups

To explore differences in biological behavior among IRG clusters, we searched for differentially expressed genes (DEGs) between groups and performed GO and KEGG enrichment analyses. The findings revealed that DEGs in CC samples were primarily enriched in immune function, particularly "T cell activation", "leukocyte cell-cell adhesion", "immune receptor activity", "MHC protein complex binding", "cytokine receptor activity", and other activities (Figure 4A). According to KEGG enrichment analysis, differential genes upregulated "Cytokine-cytokine receptor interaction", "Chemokine signaling pathway", and other pathways (Figure 4B). Next, we performed a KEGG-related GSVA analysis. The findings revealed that the "T-cell receptor signaling pathway", "B-cell receptor signaling pathway", and "JAK/STAT signaling pathway" were significantly upregulated in IRG clustering groups A and B (Figures 4C–E).

Model Construction and Validation Based on IPGs

Transcriptomic data from the TCGA and GEO cohorts screened for cervical cancer samples were matched to survival data. Sankey plots were used to show IRG clustering grouping, risk, and survival outcome (Figure 5A).

A Cox regression analysis was used for the initial screening of IRG (Supplementary Figure 2). By using LASSO regression, four significant genes were evaluated (Figures 5B and C). From the risk scores of the four IPGs, the median score was calculated (risk score = PDIA3 × 1.1277967 + CASP8 × 0.4558879 + IL1B × 0.3471111 + LY96 × −0.4902444), separating CC patients into low-risk and high-risk groups.

Furthermore, we investigated the relationship between risk scores and the two clustering subgroups, and the results revealed significant differences in risk scores among the various clustering subgroups. The median risk score in group A was higher than in IRG clustering group B, and the prognosis was worse in group A than in group B (Figure 5D). The expression of IRG varied significantly amongst risk groupings (Figure 5E). Next, CC patient samples from the TCGA and GEO cohorts were used as the train and test sets, respectively. The findings showed that the prognosis of patients in the low-risk group was superior to that of patients in the high-risk group ($p < 0.001$, Figure 5F). We also performed a survival analysis in the test set to assess the predictive prognostic consistency of the risk score (Figure 5G). The sensitivity and specificity of the ROC assessment of the prognostic model were also consistent (Figures 5H and I), indicating that the risk score is a more reliable predictor of prognosis in CC (all AUCs for survival exceeded 0.6).

IPGs-Risk Score Model for Predicting Patient Prognosis

Patients in the experimental and test groups were at increasing risk from left to right according to the median of the risk score formula. In both the experimental and test groups, the risk score increased, the number of deaths increased, and the prognosis of patients worsened (Figures 6A–F). Based on the TCGA dataset, column line plots with risk groups and clinicopathological factors comprising prognostic IPGs features were created in consideration of the problematic practical use of these features in predicting the survival of CC patients. The risk score was an independent predictor of a poor prognosis in CC, according to results of univariate and multivariate Cox regression studies (hazard ratio (HR) = 1.059, 95% confidence interval (CI): 1.134–1.084, Figure 6G) (HR = 1.058, 95% CI: 1.033–1.063, Figure 6H). Furthermore, patient age and stage were also independent prognostic factors for poor CC outcomes.

Molecular Characterization of Different IPGs-Risk Groups

The TME differed between the high-risk and low-risk groups. The high-risk and low-risk groups had significantly different StromalScore, ImmuneScore, and ESTIMATEScore scores, with the high-risk group having lower scores than the low-risk group. Furthermore, as risk scores increased, the majority of immune cell infiltration decreased (Figures 7A and B). In the radar plot, the number of immune cells in the high-risk group was significantly lower than in the low-risk group (Figure 7C). Based on these findings, it is speculated that the prognostic value of the IPGs risk score may be due to poorer immunosuppression or the promotion of invasive tumor growth. The distribution of somatic mutations in the high-risk and low-risk groups differed, and the top 20 genes with the highest mutation frequency were presented (Figures 7D and E).

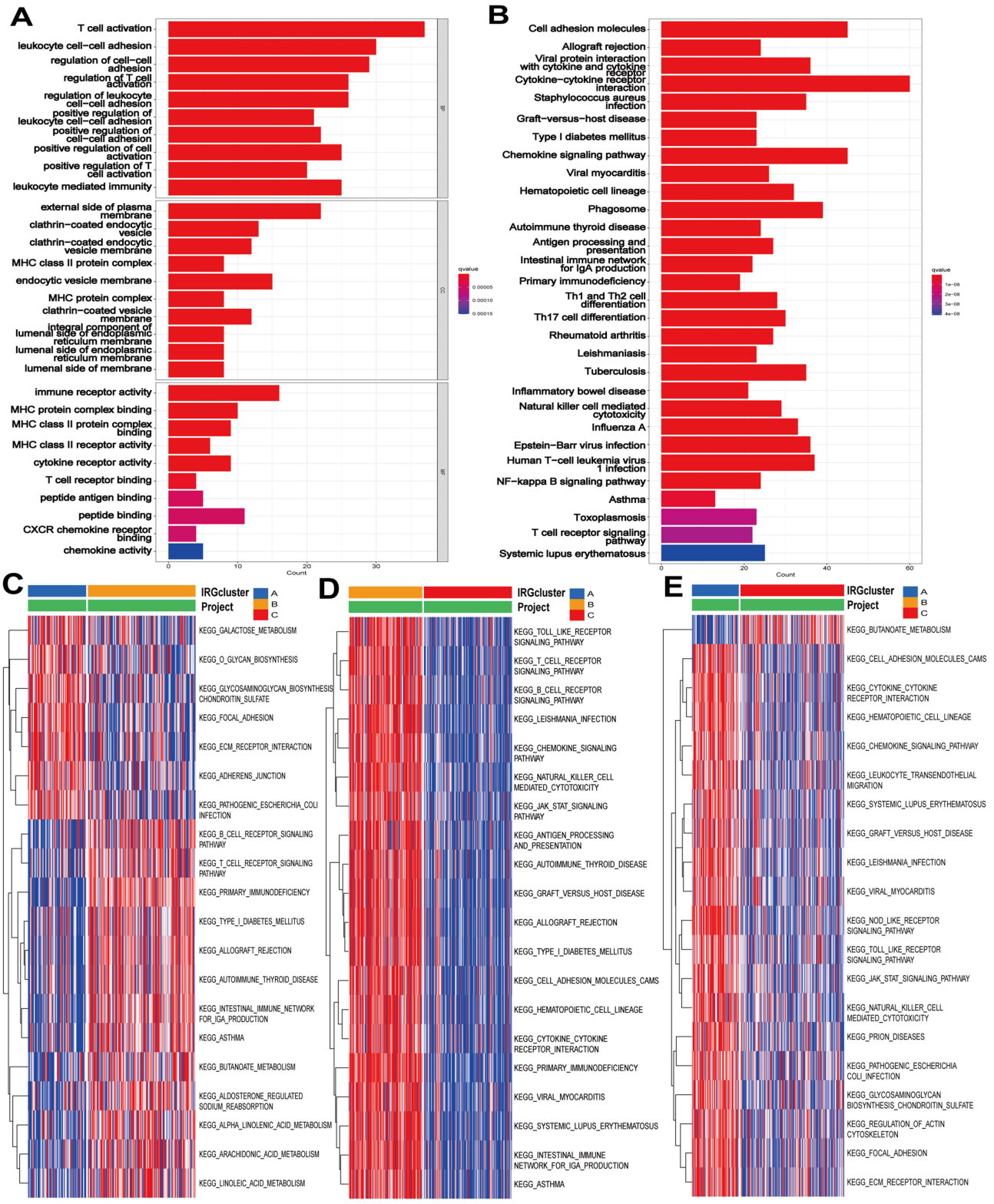

Figure 4 Comparative functional enrichment study of genes with differential expression (DEGs). (**A**) Gene Ontology enrichment analysis of DEGs, including BP, CC, and MF. (**B**) Kyoto Encyclopedia of Genes and Genomes (KEGG) enrichment analysis of DEGs. (**C**–**E**) GSEA enrichment of KEGG pathway in DEGs clustering groups A and B, B and C, and A and C, respectively.

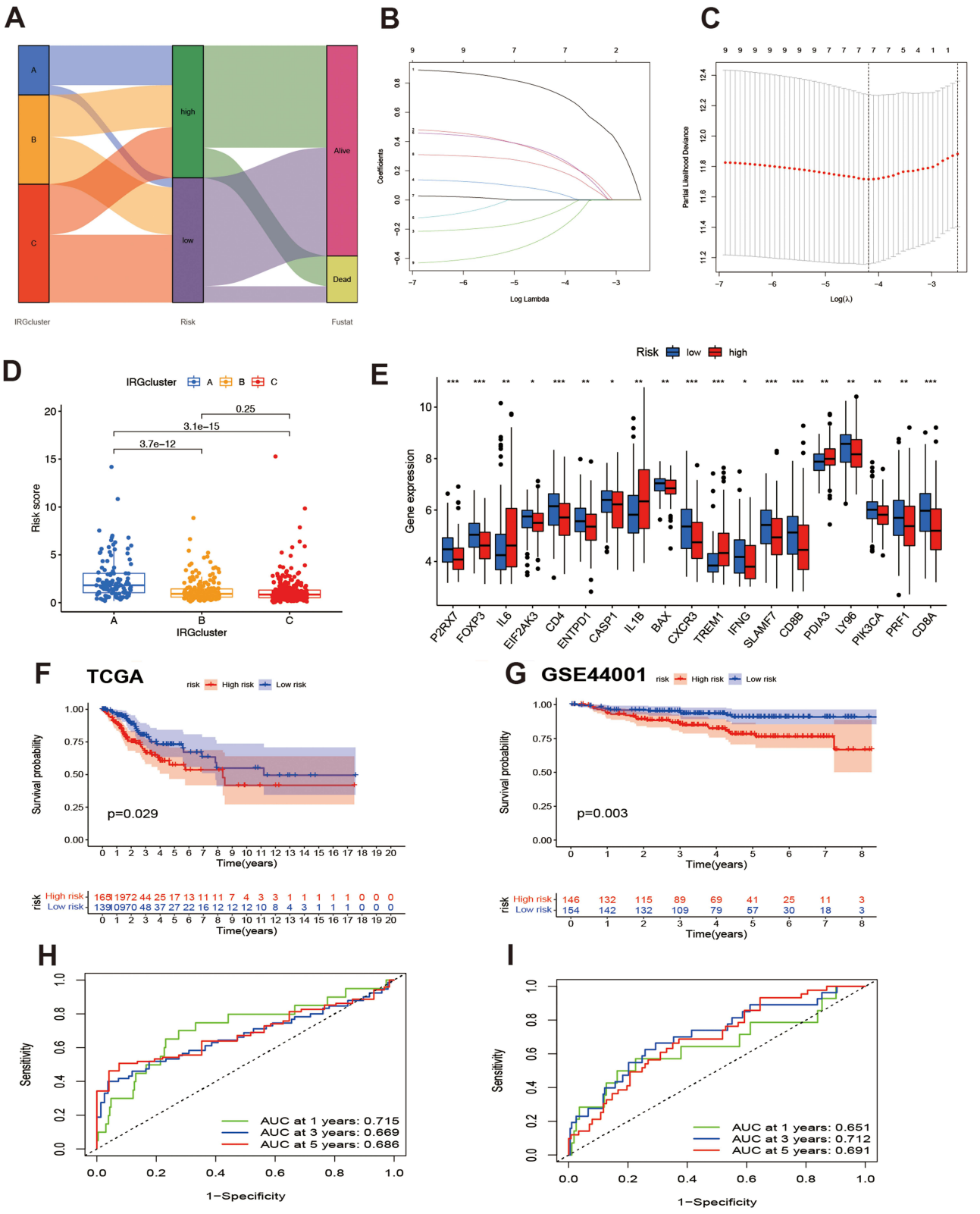

Figure 5 Construction of an immunogenic cell death prognostic genes (IPGs)-based survival model for prognosis prediction of CC. (**A**) Sankey diagram showing the distribution of immunogenic death-related genes (IRG) clustering groups, risk, and survival outcomes. (**B**) The least absolute shrinkage and selection operator (LASSO) regression of IPGs. (**C**) Cross-validation for adjusting the parameter selection in the LASSO regression. (**D**) Differences in risk scores among patients in the three IRG clustering groups ($p < 0.05$). (**E**) Differences in IRG expression in the high-risk and low-risk groups (*$p < 0.05$, **$p < 0.01$, and ***$p < 0.001$). (**F** and **G**) Kaplan–Meier survival curves in patients with CC in the experimental group (**F**) and test group (**G**) ($p < 0.05$). (**H** and **I**) The receiver operator characteristics curves showed the predictive efficiency of risk scores in the Cancer Genome Atlas (TCGA) cohort experimental group (**H**), and the Gene Expression Omnibus (GEO) cohort test group (**I**).

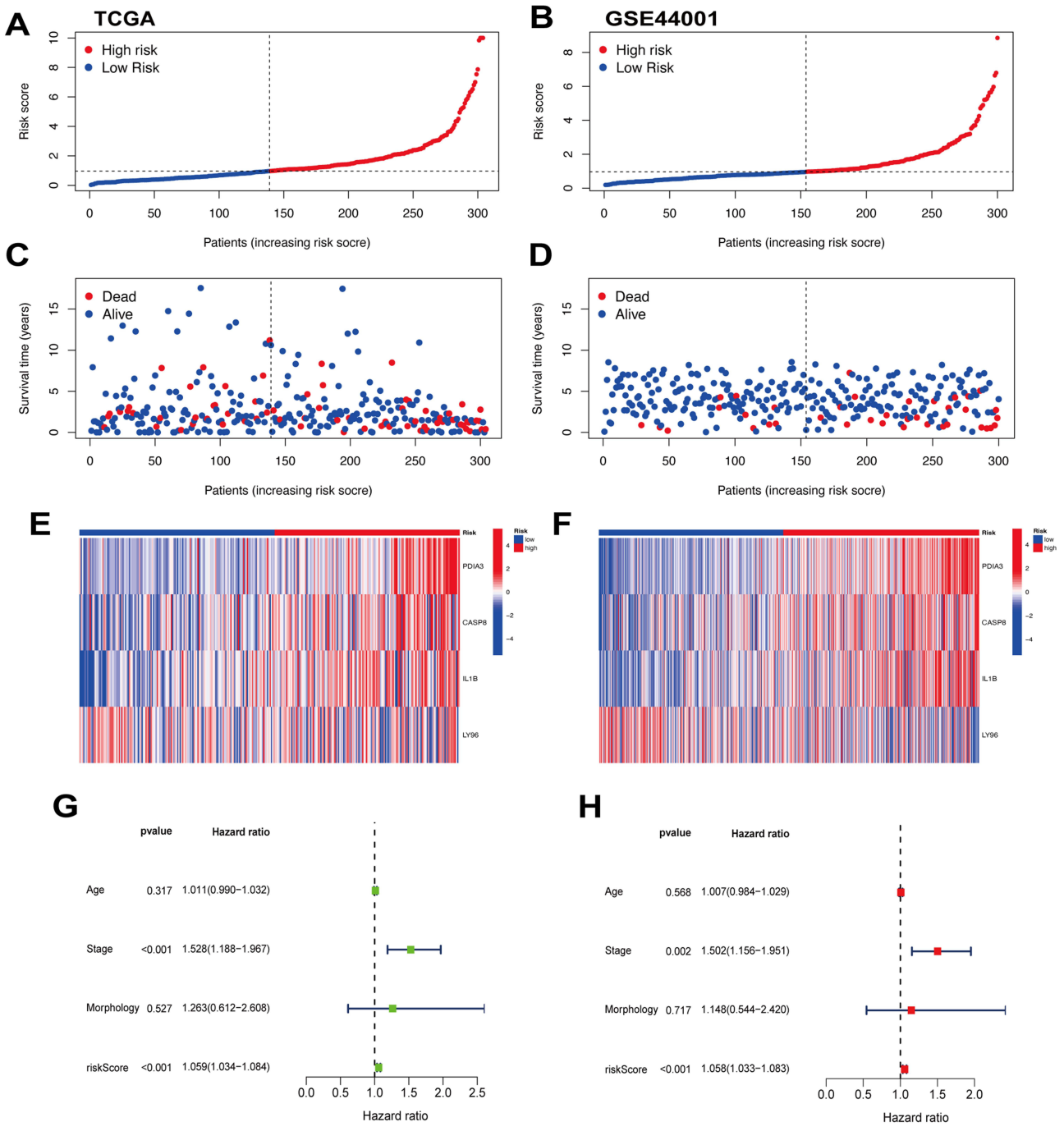

Figure 6 Prognostic analysis of the 4-gene signature model. (**A** and **B**) Distribution of patients in the Cancer Genome Atlas (TCGA) and Gene Expression Omnibus (GEO) cohort experimental groups based on risk scores. (**C** and **D**) Survival status of each patient in the TCGA and GEO cohorts. (**E** and **F**) Expression of prognostic genes in the high-risk and low-risk groups of the TCGA and GEO cohorts. (**G**) Univariate Cox regression analysis on CC patients. (**H**) Multivariate Cox regression analysis on CC patients.

Potential Role of IPGs Score in Treatment

Based on TIDE, MDSC, and CAF scores, to assess the probable immunotherapy response of CC patients in various IPGs risk categories. TIDE scores were lower in the high-risk group than in the low-risk TIDE group, while MDSC and CAF scores were higher in the high-risk group (Figures 8A–C).

To predict the value of chemotherapy efficacy based on risk scores, we compared the differences in sensitivity to common chemotherapeutic agents for CESC between the two groups, and the median IC50 values for gefitinib (Figure 8D) and palbociclib

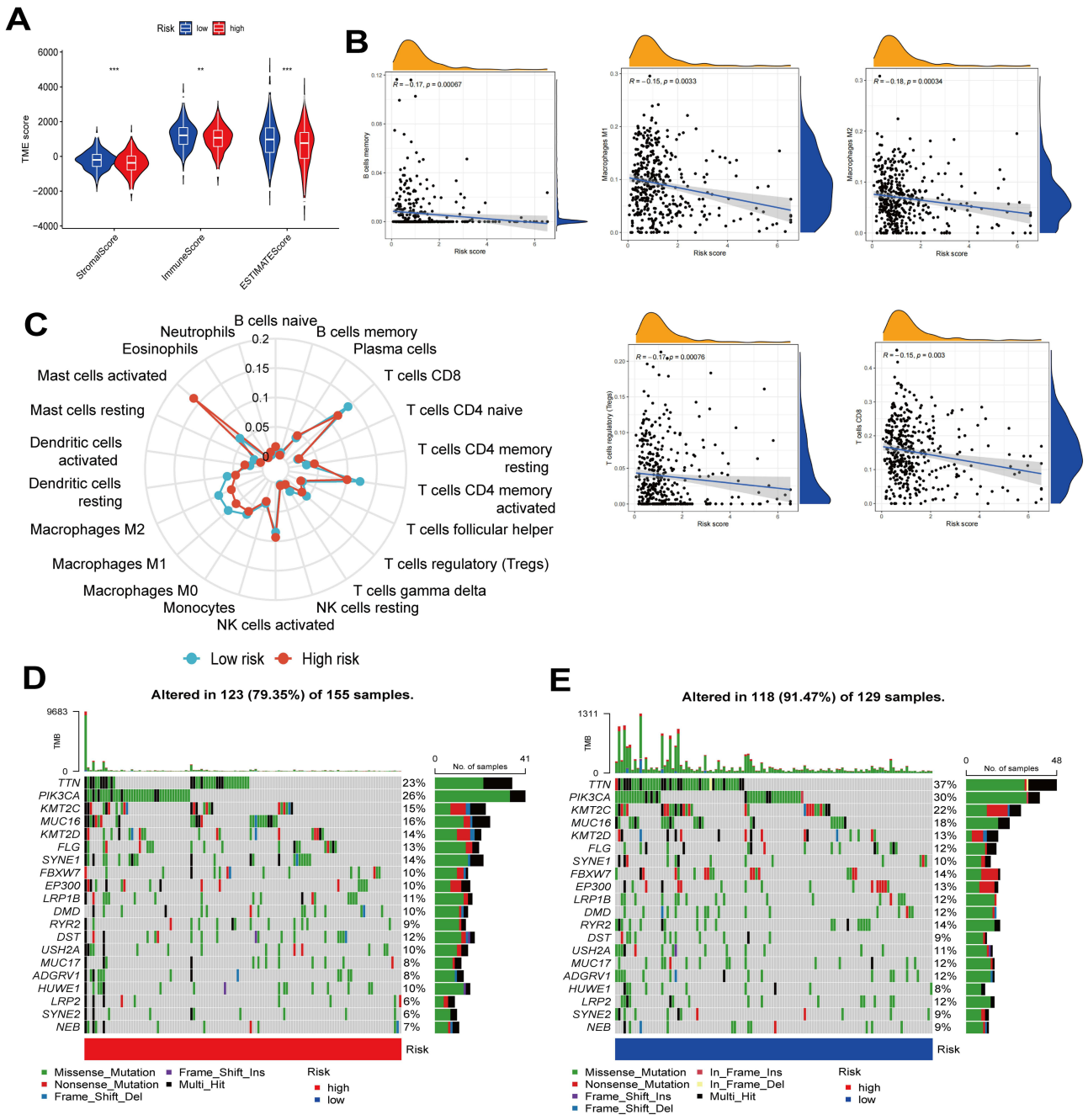

Figure 7 Comprehensive analysis of the immunogenic cell death prognostic gene scores in cervical cancer. (**A**) Tumor microenvironment differences between the high-risk and low-risk groups (**p < 0.01, and ***p < 0.001). (**B**) Correlation of immune cell infiltration risk scores. (**C**) Degree of immune cell infiltration between the high-risk and low-risk groups. (**D** and **E**) Waterfall plots show the top 20 genes with the highest mutation frequencies in the high-risk (**D**) and low-risk groups (**E**).

(Figure 8E) were significantly higher in the high-risk group than in the low-risk group ($p < 0.01$), indicating that CESC patients in the high-risk group were more sensitive to these agents. However, the median IC50 values of pyrimethamine (Figure 8F), rapamycin (Figure 8G), and sorafenib (Figure 8H) were all significantly lower in the high-risk group than in the low-risk group ($p < 0.01$), indicating that CESC patients in the low-risk group were more sensitive to these drugs.

Identification of PDIA3 as a Prognostic Key Gene

At the single-cell level, we examined the levels of IPGs expression in the microenvironment of cervical cancer, which included immune cells, stromal cells, malignant cells, and functional cells. The findings also revealed that PDIA3 was more likely to be

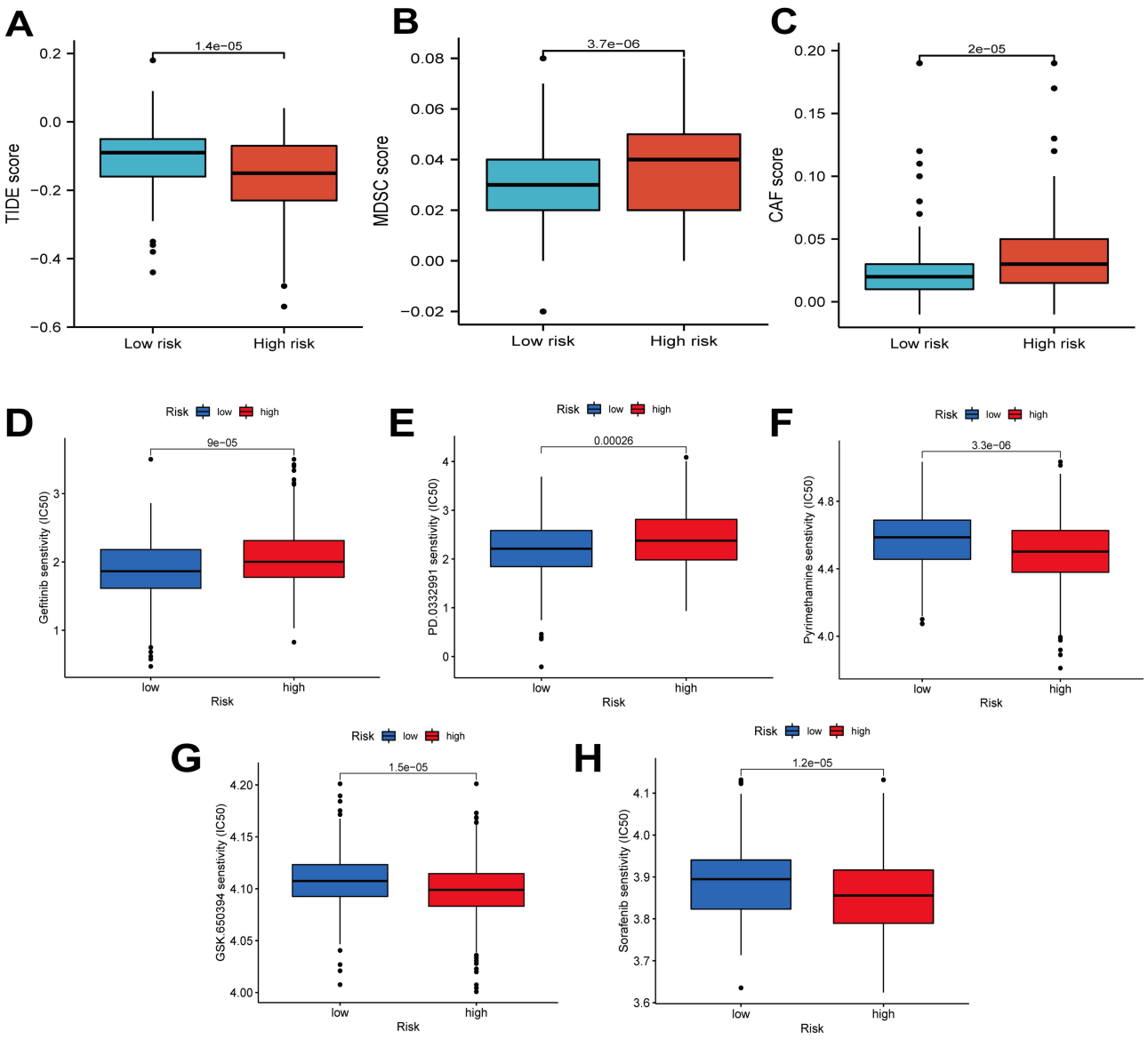

Figure 8 Role of immunogenic cell-death-related prognostic genes (IPGs) score in anti-tumor therapy. (**A**–**C**) TIDE, MDSC, and CAF scores among different IPGs' risk groups. (**D**–**H**) Differences in immunomodulatory drug sensitivity between the high-risk and low-risk groups. Gefitinib (**D**), palbociclib (**E**), pyrimethamine (**F**), rapamycin (**G**), and sorafenib (**H**).

expressed in malignant cells (Figures 9A and B). Additionally, in another dataset, IPGs between HPV16 and HPV18-positive cervical cancer patients and normal subjects were discovered to differ (Figure 9C). Cox survival analysis showed that high PDIA3 expression was the most significant adverse prognostic factor for ICD in patients with CC (HR = 1.867; Figure 9D), and PDIA3 expression was increased in cancerous tissue samples (Figure 9E). High PDIA3 expression was significantly negatively correlated with overall and progression-free survival ($p < 0.01$) (Figures 9F and G). The expression of PDIA3 in cervical squamous carcinoma and adenocarcinoma was significantly higher than in normal cervical tissues in an immunohistochemical analysis of the Human Protein Atlas. Overall, the PDIA3 gene may act as a risk factor and marker for CC patients' prognosis (Figures 9H–J).

PDIA3 is Upregulated in CC Tissues and is a Promising Diagnostic and Prognostic Biomarker

The PDIA3 expression level was examined using Western blot on CC cell lines and found to be expressed in all four cell lines at the protein level, with Hela cells being the most abundant and ME180 cells being the least abundant (Figures 10A and B). Immunofluorescence and immunohistochemistry analysis revealed that the PDIA3 protein was primarily

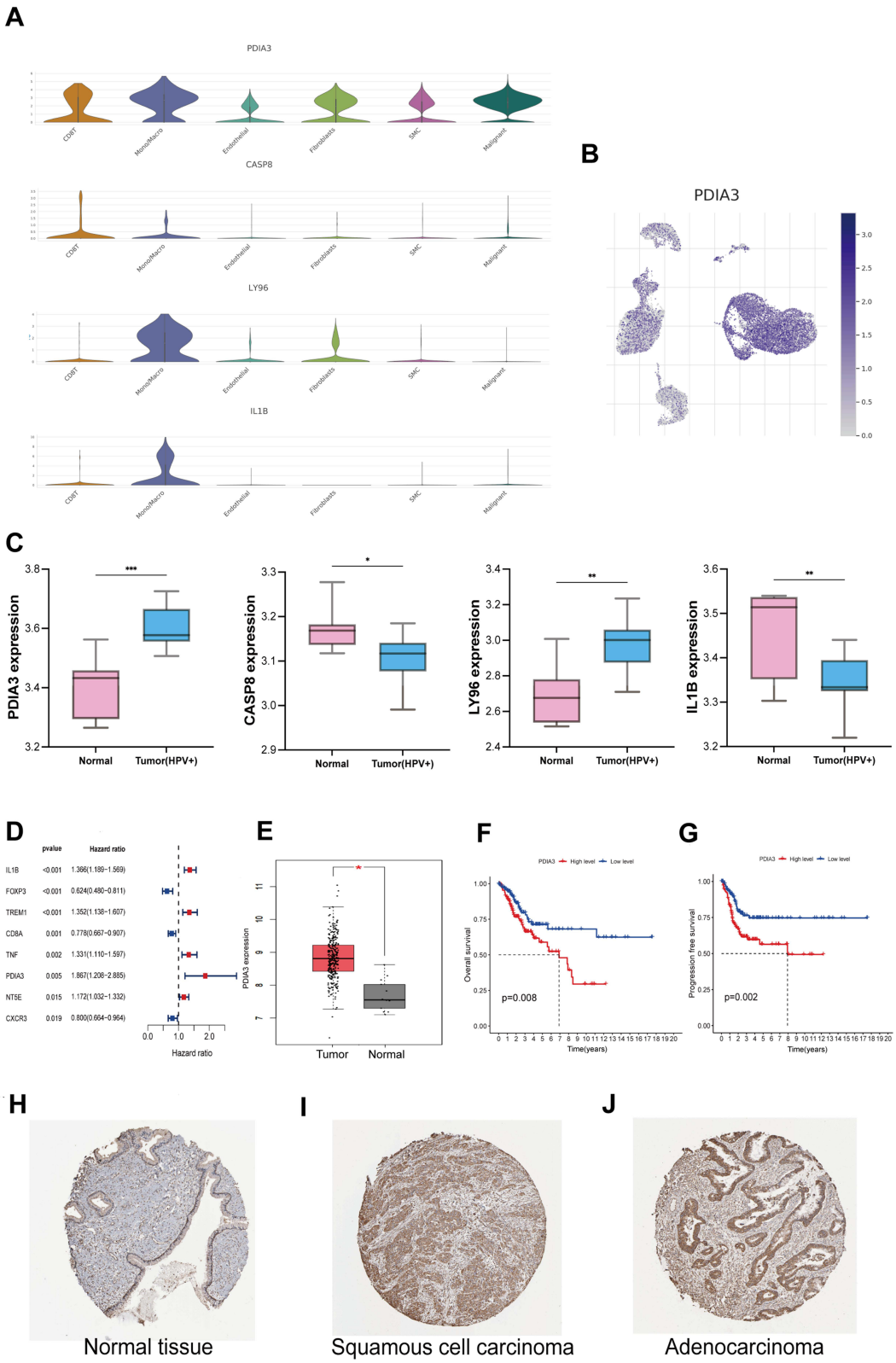

Figure 9 Expression of the PDIA3 gene in cervical cancer (CC) and its prognostic value. (**A**) The cell types of IPGs distribution in the single-cell analysis of the GSE168652 database were described. (**B**) UMAP visualization of PDIA3 in major cell subpopulations of cervical cancer. (**C**) The expression levels of HPV16- and HPV18-positive groups were compared with normal groups in the GSE6791 database (*$p < 0.05$, **$p < 0.01$, and ***$p < 0.001$). (**D**) Cox survival analysis showing hazard ratios for different IPGs. (**E**) Differences in PDIA3 expression between normal and cancer tissue samples (*$p < 0.05$). (**F** and **G**) Kaplan–Meier curves showing differences in overall survival (**F**) and progression-free survival (**G**) between PDIA3 high and low expression groups; (**H–J**) PDIA3 protein expression in normal cervical tissue samples and CC tissue samples. Normal cervical tissue (**H**), cervical squamous cancer (**I**), and cervical adenocarcinoma tissue (**J**).

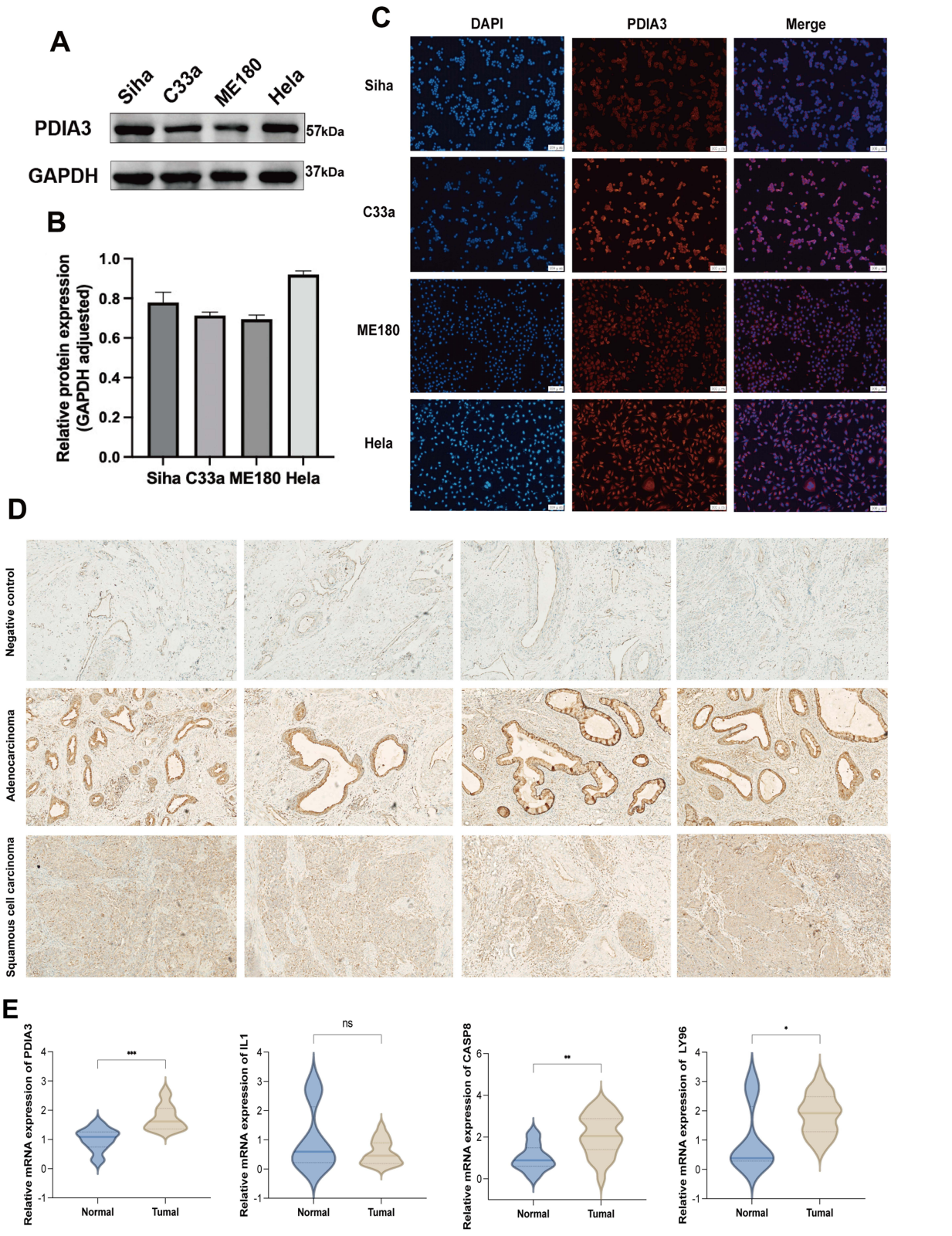

Figure 10 PDIA3 is highly expressed in cervical cancer (CC) tissues and cell lines. (**A** and **B**) Western blot analysis reveals a high expression of PDIA3 in CC cell lines. (**C**) Distribution of PDIA3 in CC cell lines. (**D**) Immunohistochemistry reveals PDIA3 expression in CC tissues, with normal cervical tissue serving as a positive control (200×). (**E**) IPGs mRNA expression relative to GAPDH in cervical cancer samples comparing (*$p < 0.05$, **$p < 0.01$, and ***$p < 0.001$).

expressed in the cytoplasm and, to a lesser extent, in the nucleus of CC cells. However, the expression was lower in normal cervical tissues, which was consistent with the results verified by the HPA database (Figures 10C and D). This suggests that PDIA3 may be a promising prognostic indicator for patients with CC. The expression levels of PDIA3, CASP8, and LY96 were significantly higher in cervical cancer samples than in normal tissue samples, but the expression levels of IL1 were not significantly different between the two groups (Figure 10E).

Discussion

Immunotherapy has emerged as a novel therapeutic pathway that benefits many cancer patients[28–30] The therapeutic efficacy of immunotherapy is determined by the synergistic action of immune cells on the tumor to control tumor growth and the modulatory effects of innate and adaptive immune cells.[31] The therapeutic impact of immunotherapy is dependent on the function of innate and adaptive immune cell control. The mode of ICD triggers not only adaptive immunity but also activates innate immunity, the process by which tumor cells are transformed from non-immunogenic to immunogenic to mediate the body's anti-tumor immune response while dying from external stimuli.[32] These substances are known as damage-associated molecular patterns (DAMPs). DAMPs generated during ICD can bind to pattern recognition receptors on the surface of DCs, causing a sequence of cytological reactions that eventually lead to the activation of innate and adaptive immune responses.[4] The immune responses triggered by anti-cancer-targeted drugs developed to study the ICD pathway of CC are expected to result in the desired therapeutic outcome.[3,33] However, the mechanism of action of ICD in CC remains unclear, so an in-depth study of its molecular mechanism will be necessary to guide CC patients' anti-cancer treatment.

This study identified three distinct patterns of ICD (IRG clustering groups A–C) based on 49 ICD-associated genes. Patients in groups A and B had more advanced immune infiltration and a worse prognosis than patients in group C. Different cellular ICD subtype features were enriched in "T cell activation", "leukocyte cell-cell adhesion", "immune receptor activity", "MHC protein complex binding", and other immune activations and are significantly associated with immune-related biological pathways. In comparison to normal cells, the surface of tumor cells, apoptotic cells, and some cells that have been treated with drugs (such as anthracyclines) produce more calreticulin. These cells' calreticulin can attach to the CD91/LRP1 receptor on the surface of various intrinsic immune cells, including macrophages, dendritic cells, and other immune cells, increasing the immune system's reaction to these cells.[34] The highly infiltrative tumor immune microenvironment and various regulatory factors have been reported to influence patient disease progression and treatment effectiveness.[35] For example, group B regulatory T cells (Tregs) are heavily infiltrated and are associated with immune-related biological pathways. High infiltration of group B Treg is associated with a poor patient prognosis.[36] Macrophages suppress the organism's immune response and remodel the stroma.[37] The JAK/STAT signaling pathway is differentially enriched between groups and is believed to be one of the most critical pathways mediating cell development and function in innate and adaptive immunity. The pathway's activation is inextricably linked to tumor development, and STAT overactivity can drive classical oncogenic signals (eg, BCR-ABL, Ras, and Src) to promote tumor growth.[38–40] The findings suggest that IRG can be used to predict clinical prognosis and immune efficacy in patients with CC. For the diagnosis and treatment of the condition, CC screening and risk assessment are crucial. Therefore, we constructed a reliable and valid risk score for the IPGs model and validated its predictive power. According to survival curves, patients with higher risk scores have significantly worse clinical outcomes, whereas patients with lower IPGs have a better prognosis. In addition, univariate and multivariate Cox regression studies showed that the IPGs model was an independent predictive variable for CC. The analysis of expression in HPV16- and HPV18-positive patients also revealed that IPGs differed between normal and cervical cancer patients, suggesting that bivalent HPV vaccination may have a preventive effect. In conclusion, it has been well demonstrated through investigation using various databases and clinical samples that the IPGs signature of CC has good predictive and independent prognostic significance.

ICD groups A and B, which have immunosuppressive effects, were associated with higher risk scores for IPGs, whereas ICD group C, which has immune-activating effects, was associated with lower risk scores for IPGs. Group C was associated with lower risk scores, indicating that higher infiltration of B memory cells, CD8+ T cells, and gamma-delta T cells play a crucial role in immune defense. The immune system's protection relies heavily on gamma-delta

T cells. Gamma-delta T cells can function as a functional link between these two important immune systems to influence tumor killing since they exhibit innate and adaptive immune systems. They are particularly important in cervical carcinogenesis and early persistent HPV infection.[41] B cells were able to stimulate B cell maturation and activation with anti-PD-L1 immunotherapy, and they predicted a significant survival advantage for HPV-infected patients.[42] This suggests that patients with low scores can benefit from the anti-tumor immune defense. The high-risk group activated considerably more mast cells than the low-risk score group. One of the primary characteristics of tumors is a chronic low-level inflammatory response, and mast cells play a very broad function as regulators of acquired immunity and innate immunity monitors.[43] Mast cells are among the first immune cells to be recruited to tumor tissue and to generate an immune response to the tumor.[44] Mast cells play a role in the expression and release of the immunosuppressive mast cells are immunosuppressive because they express and release the immunosuppressive factor IL-10, and they also affect the function of regulatory T cells (Treg) and contribute to the development of immune tolerance.[45] We found that the high-risk group had lower TIDE scores but higher MDSC and CAF scores. Higher TIDE scores indicate a greater likelihood of tumor immune escape, which is detrimental to patient prognosis.[46] According to earlier research, myeloid-derived suppressor cells (MDSCs) can severely suppress the immune cell response, and they play a crucial role in the development and spread of tumors.[47] The MDSCs can significantly suppress the immune cell response. Cancer-associated fibroblasts (CAFs) in tumor tissues promote tumor development and act as a barrier to drug and immune cell infiltration.[48] It indicates that patients in the risk group are more sensitive to immunotherapy and more likely to evade the body's immune surveillance to promote tumor development. This may be related to the property of immunogenicity, which can activate adaptive immune responses and trigger immune memory via cytotoxic T lymphocytes when malignant tumor cells appear to die.[34] Besides, somatic mutations can produce neoantigens, activate immune recognition, and kill tumor cells.[49,50] Common genes such as TTN, PIK3CA, KMT2C, and MUC16 are more frequently mutated in low-risk groups. According to the study, patients with CC who have PIK3CA mutations as a target for combination therapy can benefit from existing ERBB2/PIK3CA/AKT/mTOR targeting drugs.[51] In conclusion, the ICD prognostic risk score predicts the prognosis of CC patients and identifies patients sensitive to chemotherapeutic and immunotherapeutic agents.

We screened for PDIA3, a key poor prognostic regulator of ICD that binds to calreticulin and translocates to the cell surface, where calreticulin sends phagocytic signals to professional antigen-presenting cells, but CD47 strongly inhibits phagocytosis.[52] Furthermore, PDIA3 promotes transcriptional activator 3 (STAT3) to drive tumor development and immune escape.[53] In addition, STAT3 is involved in our enriched pathway results: the JAK/STAT signaling pathway, which is highly expressed in various malignancies.[54] STAT3 is strongly associated with poor patients' prognosis.[55] Blocking STAT3 signaling improved tumor immune escape and enhanced anti-tumor immunity.[56] These findings suggest that PDIA3 may be a potential therapeutic pathway for CC tumor treatment and a prognostic biomarker for patients.

However, there are still limitations to this study. First, the data were analyzed retrospectively in a public database, and the inclusion or exclusion of individual cases may have affected the accuracy of the results. In addition, we need to validate the model's accuracy and consistency in prognosis using more well-developed data sets. Second, additional ex vivo studies are needed to demonstrate the mechanism of IRG action in CC.

Conclusions

In conclusion, this study explored the relationship between CC prognosis and ICD using four IPGs. By exploring their biobehavioral characteristics and clinical factors, IPGs' risk scores can be used as biomarkers of prognosis and immune efficacy in CC patients. The key gene PDIA3 also has significant prognostic and diagnostic value. The potent role of ICD on tumor immunomodulation provides the foundation and new ideas for CC immunotherapy and early tumor screening strategies.

Abbreviations

ICD, Immunogenic cell death; CC, cervical cancer; TCGA, The Tumor Genome Atlas; IPGs, Immunogenic cell death-related prognostic genes; GEO, The Gene Expression Omnibus; TME, Tumor microenvironment; HR, Hazard ratio; IRG,

Immunogenic death-related genes; DCs, Recruiting dendritic cells; CTL, Cytotoxic T lymphocyte; K-M, Kaplan-Meier; KEGG, Kyoto Encyclopedia of Genes and Genomes; LASSO, Least absolute shrinkage, and selection operator; ROC, Receiver operator characteristics; ssGSEA, Single sample gene set enrichment analysis; TIDE, Tumor Immune Dysfunction, and Exclusion; DEGs, Differentially expressed genes; CNVs, Copy number variants; DAMPs, Damage-associated molecular patterns; Tregs, Regulatory T cells; MDSCs, Myeloid-derived suppressor cells; CAFs, Cancer-associated fibroblasts.

Data Sharing Statement

The RNA sequencing profiles can be gained from The Cancer Genome Atlas (TCGA) (https://portal.gdc.cancer.gov/) and Gene Expression Omnibus (GEO) (https://www.ncbi.nlm.nih.gov/geo/). Further inquiries can be directed to the corresponding author.

Informed Consent Statement

This study was carried out in conformity with the Declaration of Helsinki, national and international regulations, and ethical standards. Both TCGA and GEO are open databases. The patients involved in the database have obtained ethical approval. Users can download relevant data for free for research and publish relevant articles. The Ethics Committee of Fujian Cancer Hospital reviewed and approved the studies involving human participants. The patients/participants provided their written informed consent to participate in this study.

Acknowledgments

This work was supported by the National Natural Science Foundation of China (81873045), Joint Funds for the Innovation of Science and Technology of Fujian province (2021Y9209), and the high-level talents training project of Fujian Cancer Hospital (2022YNG04). We are grateful for the fund.

Author Contributions

All authors made a significant contribution to the work reported, whether that is in the conception, study design, execution, acquisition of data, analysis, and interpretation, or all these areas; took part in drafting, revising, or critically reviewing the article; gave final approval of the version to be published; have agreed on the journal to which the article has been submitted; and agree to be accountable for all aspects of the work.

Funding

This work was supported by the National Natural Science Foundation of China (81873045), Joint Funds for the Innovation of Science and Technology of Fujian province (2021Y9209), and the high-level talents training project of Fujian Cancer Hospital (2022YNG04).

Disclosure

The authors declare that they have no conflicts of interest.

References

1. Sung H, Ferlay J, Siegel RL, et al. Global cancer statistics 2020: GLOBOCAN estimates of incidence and mortality worldwide for 36 cancers in 185 countries. *CA Cancer J Clin*. 2021;71(3):209–249. doi:10.3322/caac.21660
2. Liontos M, Kyriazoglou A, Dimitriadis I, Dimopoulos MA, Bamias A. Systemic therapy in cervical cancer: 30 years in review. *Crit Rev Oncol Hematol*. 2019;137:9–17. doi:10.1016/j.critrevonc.2019.02.009
3. Montico B, Nigro A, Casolaro V, Dal Col J. Immunogenic apoptosis as a novel tool for anticancer vaccine development. *Int J Mol Sci*. 2018;19 (2):594. doi:10.3390/ijms19020594
4. Fucikova J, Kepp O, Kasikova L, et al. Detection of immunogenic cell death and its relevance for cancer therapy. *Cell Death Dis*. 2020;11(11):1013. doi:10.1038/s41419-020-03221-2
5. Baines AC, Ershler R, Kanapuru B, et al. FDA approval summary: belantamab mafodotin for patients with relapsed or refractory multiple myeloma. *Clin Cancer Res*. 2022;28(21):4629–4633. doi:10.1158/1078-0432.CCR-22-0618

6. Singh S, Jaigirdar AA, Mulkey F, et al. FDA approval summary: lurbinectedin for the treatment of metastatic small cell lung cancer. *Clin Cancer Res*. 2021;27(9):2378–2382. doi:10.1158/1078-0432.CCR-20-3901
7. Johnson WE, Li C, Rabinovic A. Adjusting batch effects in microarray expression data using empirical Bayes methods. *Biostatistics*. 2007;8 (1):118–127. doi:10.1093/biostatistics/kxj037
8. Garg AD, De Ruysscher D, Agostinis P. Immunological metagene signatures derived from immunogenic cancer cell death associate with improved survival of patients with lung, breast or ovarian malignancies: a large-scale meta-analysis. *Oncoimmunology*. 2016;5(2):e1069938.
9. Li Y, Zhang H, Li Q, et al. CDK12/13 inhibition induces immunogenic cell death and enhances anti-PD-1 anticancer activity in breast cancer. *Cancer Lett*. 2020;495:12–21. doi:10.1016/j.canlet.2020.09.011
10. Lotsberg ML, Wnuk-Lipinska K, Terry S, et al. AXL targeting abrogates autophagic flux and induces immunogenic cell death in drug-resistant cancer cells. *J Thorac Oncol*. 2020;15(6):973–999. doi:10.1016/j.jtho.2020.01.015
11. Roh SA, Kwon YH, Lee JL, Kim SK, Kim JC. SLAMF7 and TREM1 mediate immunogenic cell death in colorectal cancer cells: focus on microsatellite stability. *Anticancer Res*. 2021;41(11):5431–5444. doi:10.21873/anticanres.15355
12. Araki K, Yamamuro N, Tomonobu N, Kumon H. REIC/Dkk-3 gene therapy induces immunogenic cell death in a mouse model of malignant mesothelioma. *Anticancer Res*. 2021;41(10):4837–4855. doi:10.21873/anticanres.15298
13. Zhang H, Meltzer P, Davis S. RCircos: an R package for circos 2D track plots. *BMC Bioinform*. 2013;14:244. doi:10.1186/1471-2105-14-244
14. Mayakonda A, Lin DC, Assenov Y, Plass C, Koeffler HP. Maftools: efficient and comprehensive analysis of somatic variants in cancer. *Genome Res*. 2018;28(11):1747–1756. doi:10.1101/gr.239244.118
15. Wilkerson MD, Hayes DN. ConsensusClusterPlus: a class discovery tool with confidence assessments and item tracking. *Bioinformatics*. 2010;26 (12):1572–1573. doi:10.1093/bioinformatics/btq170
16. Liu J, Geng R, Ni S, et al. Pyroptosis-related lncRNAs are potential biomarkers for predicting prognoses and immune responses in patients with UCEC. *Mol Ther Nucleic Acids*. 2022;27:1036–1055. doi:10.1016/j.omtn.2022.01.018
17. Yu G, Wang LG, Han Y, He QY. clusterProfiler: an R package for comparing biological themes among gene clusters. *Omics*. 2012;16(5):284–287. doi:10.1089/omi.2011.0118
18. Ritchie ME, Phipson B, Wu D, et al. limma powers differential expression analyses for RNA-sequencing and microarray studies. *Nucleic Acids Res*. 2015;43(7):e47. doi:10.1093/nar/gkv007
19. Engebretsen S, Bohlin J. Statistical predictions with glmnet. *Clin Epigenetics*. 2019;11(1):123. doi:10.1186/s13148-019-0730-1
20. Tibshirani R. The lasso method for variable selection in the cox model. *Stat Med*. 1997;16(4):385–395. doi:10.1002/(SICI)1097-0258(19970228)16:4<385::AID-SIM380>3.0.CO;2-3
21. Sotiriou C, Wirapati P, Loi S, et al. Gene expression profiling in breast cancer: understanding the molecular basis of histologic grade to improve prognosis. *J Natl Cancer Inst*. 2006;98(4):262–272. doi:10.1093/jnci/djj052
22. Heagerty PJ, Zheng Y. Survival model predictive accuracy and ROC curves. *Biometrics*. 2005;61(1):92–105. doi:10.1111/j.0006-341X.2005.030814.x
23. Laska E, Meisner M, Wanderling J. A maximally selected test of symmetry about zero. *Stat Med*. 2012;31(26):3178–3191. doi:10.1002/sim.5384
24. Charoentong P, Finotello F, Angelova M, et al. Pan-cancer immunogenomic analyses reveal genotype-immunophenotype relationships and predictors of response to checkpoint blockade. *Cell Rep*. 2017;18(1):248–262. doi:10.1016/j.celrep.2016.12.019
25. Liu J, Chen C, Wang Y, et al. Comprehensive of N1-methyladenosine modifications patterns and immunological characteristics in ovarian cancer. *Front Immunol*. 2021;12:746647. doi:10.3389/fimmu.2021.746647
26. Hänzelmann S, Castelo R, Guinney J. GSVA: gene set variation analysis for microarray and RNA-seq data. *BMC Bioinform*. 2013;14:7. doi:10.1186/1471-2105-14-7
27. Geeleher P, Cox N, Huang RS, Barbour JD. pRRophetic: an R package for prediction of clinical chemotherapeutic response from tumor gene expression levels. *PLoS One*. 2014;9(9):e107468. doi:10.1371/journal.pone.0107468
28. Riley RS, June CH, Langer R, Mitchell MJ. Delivery technologies for cancer immunotherapy. *Nat Rev Drug Discov*. 2019;18(3):175–196. doi:10.1038/s41573-018-0006-z
29. Ji H, Ren M, Liu T, Sun Y, Wang F. Prognostic and immunological significance of CXCR2 in ovarian cancer: a promising target for survival outcome and immunotherapeutic response assessment. *Dis Markers*. 2021;2021:5350232. doi:10.1155/2021/5350232
30. Lin L, Chen L, Xie Z, Chen J, Li L, Lin A. Identification of NAD(+) metabolism-derived gene signatures in ovarian cancer prognosis and immunotherapy. *Front Genet*. 2022;13:905238. doi:10.3389/fgene.2022.905238
31. Zhang Y, Zhang Z. The history and advances in cancer immunotherapy: understanding the characteristics of tumor-infiltrating immune cells and their therapeutic implications. *Cell Mol Immunol*. 2020;17(8):807–821. doi:10.1038/s41423-020-0488-6
32. Kroemer G, Galluzzi L, Kepp O, Zitvogel L. Immunogenic cell death in cancer therapy. *Annu Rev Immunol*. 2013;31(1):1–72. doi:10.1146/annurev-immunol-032712-100008
33. Ahmed A, Tait SWG. Targeting immunogenic cell death in cancer. *Mol Oncol*. 2020;14(12):2994–3006. doi:10.1002/1878-0261.12851
34. Kroemer G, Galassi C, Zitvogel L, Galluzzi L. Immunogenic cell stress and death. *Nat Immunol*. 2022;23(4):487–500. doi:10.1038/s41590-022-01132-2
35. Quail DF, Joyce JA. Microenvironmental regulation of tumor progression and metastasis. *Nat Med*. 2013;19(11):1423–1437. doi:10.1038/nm.3394
36. Zimmer N, Trzeciak ER, Graefen B, Satoh K, Tuettenberg A. GARP as a therapeutic target for the modulation of regulatory T cells in cancer and autoimmunity. *Front Immunol*. 2022;13:928450. doi:10.3389/fimmu.2022.928450
37. Pan Y, Yu Y, Wang X, Zhang T. Tumor-associated macrophages in tumor immunity. *Front Immunol*. 2020;11:583084. doi:10.3389/fimmu.2020.583084
38. Villarino AV, Kanno Y, Ferdinand JR, O'Shea JJ. Mechanisms of Jak/STAT signaling in immunity and disease. *J Immunol*. 2015;194(1):21–27. doi:10.4049/jimmunol.1401867
39. Verhoeven Y, Tilborghs S, Jacobs J, et al. The potential and controversy of targeting STAT family members in cancer. *Semin Cancer Biol*. 2020;60:41–56. doi:10.1016/j.semcancer.2019.10.002
40. Gutiérrez-Hoya A, Soto-Cruz I. Role of the JAK/STAT pathway in cervical cancer: its relationship with HPV E6/E7 oncoproteins. *Cells*. 2020;9 (10):2297. doi:10.3390/cells9102297
41. Dogan S, Terzioglu E, Ucar S. Innate immune response against HPV: possible crosstalking with endocervical γδ T cells. *J Reprod Immunol*. 2021;148:103435. doi:10.1016/j.jri.2021.103435

42. Kim SS, Shen S, Miyauchi S, et al. B cells improve overall survival in HPV-associated squamous cell carcinomas and are activated by radiation and PD-1 blockade. *Clin Cancer Res*. 2020;26(13):3345–3359. doi:10.1158/1078-0432.CCR-19-3211
43. De toledo MAS, Fu X, Maié T, et al. KIT D816V mast cells derived from induced pluripotent stem cells recapitulate systemic mastocytosis transcriptional profile. *Int J Mol Sci*. 2023;24(6):1.
44. Crusz SM, Balkwill FR. Inflammation and cancer: advances and new agents. *Nat Rev Clin Oncol*. 2015;12(10):584–596. doi:10.1038/nrclinonc.2015.105
45. Liu Z, Zhou Q, Wang Z, et al. Intratumoral TIGIT + CD8 + T-cell infiltration determines poor prognosis and immune evasion in patients with muscle-invasive bladder cancer. *J Immunother Cancer*. 2020;8(2):e000978. doi:10.1136/jitc-2020-000978
46. Jiang P, Gu S, Pan D, et al. Signatures of T cell dysfunction and exclusion predict cancer immunotherapy response. *Nat Med*. 2018;24(10):1550–1558. doi:10.1038/s41591-018-0136-1
47. Groth C, Hu X, Weber R, et al. Immunosuppression mediated by myeloid-derived suppressor cells (MDSCs) during tumour progression. *Br J Cancer*. 2019;120(1):16–25. doi:10.1038/s41416-018-0333-1
48. Chen X, Song E. Turning foes to friends: targeting cancer-associated fibroblasts. *Nat Rev Drug Discov*. 2019;18(2):99–115. doi:10.1038/s41573-018-0004-1
49. Smith CC, Selitsky SR, Chai S, Armistead PM, Vincent BG, Serody JS. Alternative tumour-specific antigens. *Nat Rev Cancer*. 2019;19(8):465–478. doi:10.1038/s41568-019-0162-4
50. Turajlic S, Litchfield K, Xu H, et al. Insertion-and-deletion-derived tumour-specific neoantigens and the immunogenic phenotype: a pan-cancer analysis. *Lancet Oncol*. 2017;18(8):1009–1021. doi:10.1016/S1470-2045(17)30516-8
51. Zammataro L, Lopez S, Bellone S, et al. Whole-exome sequencing of cervical carcinomas identifies activating ERBB2 and PIK3CA mutations as targets for combination therapy. *Proc Natl Acad Sci U S A*. 2019;116(45):22730–22736. doi:10.1073/pnas.1911385116
52. Kepp O, Senovilla L, Vitale I, et al. Consensus guidelines for the detection of immunogenic cell death. *Oncoimmunology*. 2014;3(9):e955691. doi:10.4161/21624011.2014.955691
53. Li Y, Song Z, Han Q, et al. Targeted inhibition of STAT3 induces immunogenic cell death of hepatocellular carcinoma cells via glycolysis. *Mol Oncol*. 2022;16(15):2861–2880. doi:10.1002/1878-0261.13263
54. Yu H, Pardoll D, Jove R. STATs in cancer inflammation and immunity: a leading role for STAT3. *Nat Rev Cancer*. 2009;9(11):798–809. doi:10.1038/nrc2734
55. Aggarwal BB, Kunnumakkara AB, Harikumar KB, et al. Signal transducer and activator of transcription-3, inflammation, and cancer: how intimate is the relationship? *Ann N Y Acad Sci*. 2009;1171(1):59–76. doi:10.1111/j.1749-6632.2009.04911.x
56. Sui Q, Zhang J, Sun X, Zhang C, Han Q, Tian Z. NK cells are the crucial antitumor mediators when STAT3-mediated immunosuppression is blocked in hepatocellular carcinoma. *J Immunol*. 2014;193(4):2016–2023. doi:10.4049/jimmunol.1302389